ISSN 1682-296X (Print)
ISSN 1682-2978 (Online)

Bio Technology

ANSInet
Asian Network for Scientific Information
308 Lasani Town, Sargodha Road, Faisalabad - Pakistan

Biotechnology 4 (4): 341-346, 2005
ISSN 1682-296X

Crystallization and Structural Studies of Lysozyme from Hen Egg White, Using Vapour Diffusion Techniques

[1]C.N. Fokunang, [1]K.A. Watson, [1]A. Purvis and [2]E.A. Tembe-Fokunang
[1]Structural Biology Unit, The University of Reading,
P.O. Box 221, Whiteknights, Reading, Berkshire, RG6 6As, UK
[2]Pfizer Global Research and Development, Sandwich Laboratories, CT13 9NJ, UK

Abstract: The aim of this study was to develop an in-house high throughput method of crystallization and structure determination of lysozyme enzyme as model in structure-based drug design studies. Lysozyme stock solution at 50 mg mL^{-1} from hen egg white was crystallized using the vapour diffusion techniques in buffer A [0.1 M Na acetate/acetic acid pH 4.8, 0.2% Na azide (w/v), 1.1 M NaCl] and buffer B [0.1 M Na acetate/acetic acid pH 4.8, 0.02% Na azide (w/v), 25% ethylene glycol (w/v), 1.7 m M NaCl]. Two 24 well plates in duplicates were used for each buffer preparations and incubated at 4°C. High quality crystals between 0.2-0.5 mm sizes, were produced in buffer A plate well after days 2 of incubation and none in buffer B. The crystal data collection and refinement showed a high resolution of the outer shell of 2.28-1.92 Å, completeness of 98.7%, space group $P4_32_12$ and mosaicity of 0.415.

Key words: Hen egg white, lysozyme, X-ray crystallography

INTRODUCTION

Hen egg-white lysozyme (E.C. 3.2.1.17; HEWL) was the first enzyme to have its three-dimensional structure determined and has become the most widely studied enzymes in structural biology to date[1,2]. The lysozyme is a relatively small enzyme which dissolves certain bacteria by cleaving the polysaccharide component of their cell walls[3,4]. The enzyme from hen egg white, a rich source, is made up of a single polypeptide chain of 129 amino acids and has a mass of 14.6 kDa[5-7]. The enzyme is cross-linked by four disulphide bridges, which contribute to its high stability[8,9]. Lysozyme does not contain a prosthetic group and thus lacks a built-in marker at its active site, in contrast with such proteins as myoglobin and hemoglobin[7,10,11]. The essential information needed to identity the active site, specify the mode of binding of substrate and elucidate the enzymatic mechanism came from an X-ray crystallographic study of the interaction of lysozyme with inhibitors[9,12,13].

The aim of this study was to develop an in-house high throughput method of crystallization and structure determination of lysozyme enzyme as model in structure-based drug design studies.

MATERIALS AND METHODS

Crystallization of lysozyme: Lysozyme stock solution at 50 mg mL^{-1} in 0.1 M Na acetate/acetic acid pH 4.8, 0.02% Na azide were used for this study. Lysozyme crystallization-Buffers required was 100 mL of; Buffer A: 0.1 M Na acetate/acetic acid pH 4.8, 0.02% Na azide (w/v), 1.1 M NaCl and Buffer B: 0.1 M Na acetate/acetic acid pH 4.8, 0.02% Na azide (w/v), 25% (w/v) ethylene glycol, 1.7 m M NaCl.

Materials for lysozyme crystallization: Twenty four wells XRL plate (Molecular Dimension Ltd) were used in duplicates, silicone vacuum grease, Plastic cover slips, 22 mm, square (Molecular Dimensions Ltd), chemicals from FLUKA, Sigma and Calbiochem, Precipitant solutions, Protein solution, 50 mg mL^{-1} lysozyme from hen egg white A and buffer B above.

Crystallization by hanging drops technique: Silicone grease was piped around the rim of each well of the 24 wells, of the Linbro tray, to provide a seal with the cover slip when closing the well. The linbro 24 well were used for crystallization which were blown free of dust with pressurized air. The protein was centrifuged for 15 min at 14000 rpm at 4°C, to remove any precipitated protein. If small particles were present in the crystallization, these particles would act as seeds causing too many crystals forming.

Two 24 well plates in duplicates were used for each buffer. The plate wells were each aliquoted with 1 mL of buffer A or B. Small amount of well solution was pipetted onto cover slip, mixed with a small amount of protein

Corresponding Author: C.N. Fokunang, Structural Biology Unit, The University of Reading,
P.O. Box 221, Whiteknights, Reading, Berkshire, RG6 6As, UK

solution giving a total drop size of 4 μL, the ratio of which was varied to alter the protein concentration of the drop. The cover slip was inverted over the same well and pressed into the silicone grease to create a seal, then stored in a quiet cool room temperature of 20°C. Vapour diffusion is the most commonly employed method for growing crystals of macromolecules for X-ray structure determination[14], experimental procedure works by mixing equal volume aliquots of the macromolecules solution with a reservoir solution that is at the condition of pH, precipitant, or temperature) of interest. The mixed solution was then either placed on a pedestal or suspended from a cover slip or other surface in an enclosed volume with the reservoir of precipitant solution. The reservoir solution, having a higher solute concentration, has a lower vapour pressure than the macromolecule solution droplet. Because of this, water vapour leaving the crystallization droplet would be preferentially reabsorbed by the reservoir solution, resulting in a net transfer of water to the reservoir, until the two liquid bodies had equivalent vapour pressures. This process results in a progressive increase in the precipitant and solute concentration in the crystallization drop, hopefully leading to the desolubilization of the macromolecules in crystalline form. The plate layout for the crystallization screening is shown in Table 1.

The 24 well plates were laid out into six main well columns buffer A plate A (AO, A1, A2, A3, A4, A5), with varied well solution/protein concentration. The wells had four replicates per column.

Fine screening score: The plates were observed daily under a dissection microscope. No optimization of crystal formation condition found in the initial screen was investigated. The following scale was used to screen the crystal drops.

Drop	Score
Clear	-
Cloudy precipitate	1
Gelatinous or particulate precipitate	2
Spherullites	3
Needles	4
Plane	5
Prism	6

Data collection

Lysozyme X-ray data collection: A single well-form crystal of dimension (0.3 mm) was mounted within a loop from drop grown under [0.1 M Na acetate, 0.02% Na azide (w/v), 1.1 M NaCl adjusted to pH 4.8 with 0.1 M acetic acid], in well A42, (with drop containing 1.5 μL well solution and 2.5 protein solution) and soaked for a few seconds into a cryoprotectant buffer. The cryoprotectant

Table 1: Plate layout for lysozyme crystallization screening

Replicate	A0	A1	A2	A3	A4	A5
1	A01	A11	A21	A31	A41	A51
2	A02	A12	A22	A32	A42	A52
3	A03	A13	A23	A33	A43	A53
4	A04	A14	A24	A34	A44	A54
Protein	1 μL	1.5 μL	2.0 μL	2.0 μL	2.5 μL	3.0 μL
Buffer	3 μL	2.5 μL	2.0 μL	2.0 μL	1.5 μL	1.0 μL

Total drop size = 4 μL, well buffer = 1 mL

buffer was similar to the well solution but with addition of 20% (v/v) glycerol to stop ice formation during freezing, which may damage the crystal structure. This was transferred to the goniostat in the path of gaseous nitrogen stream at 100 K (-160°C). Alignment with the X-ray beam was done using a camera. The crystal was mounted on the goniometer and the X-ray beam directed through the collimator hit the crystal and the rays were diffracted and spots collected on the image plate which are used for data analysis.

X-ray data collection: Dataset was recorded using a Rigaku FR-D Copper rotating Anode generater, with wavelength 1.542Å. The images were collected on a Saturn 92 CCD detector. Two data sets were collected: The low resolution data set was collected with a crystal detector distance of 50 mm, oscillation of 1 and exposure time of 30 sec with total images of 59 collected. The high resolution data set was similar to the low resolution but with 60 sec exposure times.

Data processing: The Crystal Clear Program using the d*trex path was used to process the low resolution dataset to record images, find strong spots, then, autoindexed to estimate the space group and unit cell. The unit cell and space group was then used to predict location of spots. The predicted location of spots was used to refine space group, unit cell volume, unit cell length and other parameters of interest. The recorded spots were used to estimate symmetry of space group ($P4_32_12$ or $P4_12_12$), based on a positioned model, then scaling an averaging was done to produce final data used for molecular and statistics, to determine spot location and intensity, (molecular replacement was done using Molrep (CCP4 programme), for structural solving and determination of completeness, symmetry within the cell, space group, signal/noise ratio (I/σ). A high signal/noise ratio was an indication of a good data. The R factor (Rmerge) statistic data was generated for estimating agreement between model and the data set. The lower the value the better. Data reduction for the integration of intensities in a spot was done by separating the background counts from the reflection and used for the electron density map building, model construction and refinement using CCP4, CNS.

RESULTS

Lysozyme crystal screen scoring: Using the scoring scale of 1-6 described in earlier, the crystals were screened in the different well plates at daily intervals, until crystal sizes of 0.2-0.5 mm were attained. The crystal screen scores at day two and day 4 for plates A (0.1 M Na acetate, 0.02% Na azide, 1.1 M NaCl adjusted to pH 4.8 with 0.1 M acetic acid) and plate B (0.1 M Na acetate, 0.02% Na azide w/v, 25% ethylene glycol, 1.7 m M NaCl adjusted at pH 4.8 with 0.1 M acetic acid are outlined in Table 2a. On day two there was crystal formation in most of the wells, especially well A4 where the buffer/protein ratio was 1.5:2.4 μL, given a well total volume of 4 μL.

X-ray diffraction data collection: Well formed crystals more than 0.2 mm in size as shown in Fig. 1, were harvested from drops with a loop and placed in cryo-protectant buffer similar to the crystallization buffer with added 20% glycerol to prevent ice formation, then flash frozen in gaseous nitrogen and diffraction measured at 100 K (Table 3).

Fifty nine images were collected from crystal number 3 at conditions shown in Table 4.

The data collection and refinement for a single crystal form showed that the space group after molecular replacement was a tetragonal system $P4_32_12$ which was the best fit model than model $P4_12_12$ (Table 5). The unit cell dimension was (a 78.78, b 78.75 and c 37.09) and the unit cell angles were α90, β90 and γ90. The percentage completeness was 98.7%, with a total number of reflections recorded as 27553. The number of unique reflections was recorded as 6208. The outer resolution shell was 2.28-1.92Å and the Rmerge was 5.8%, with a signal noise ratio I/sig (I) of 5.8%.

Table 2: Lysozyme crystal screen scores at day two and day 4, for buffer A (0.1 M Na acetate, 0.02% Na azide, 1.1 M NaCl adjusted to pH 4.8 with 0.1 M acetic acid)

Crystal screen Plate A at day 2

Replicates	A0	A1	A2	A3	A4	A5	Observation
1	-	-	6	6	6	6	Crystals formed in
2	6	-	-	6	6	6	most well less than
3	6	-	6	6	6	X	0.2 mm in size.
4	-	6	6	1	6	6	
Buffe	3 μL	2.5 μL	2.0 μL	2.0 μL	1.5 μL	1.0 μL	
Protein	1 μL	1.5 μL	2.0 μL	2.0 μL	2.5 μL	3.0 μL	

Crystal screen Plate A at day 4

Replicates	A0	A1	A2	A3	A4	A5	Observation
1	5	-	6	6	6	6	More crystals
2	6	6	-	6	6	6	developed in wells
3	6	-	6	6	6	X	and increased size
4	6	6	6	6	6	6	greater than 0.2 mm for use in X-ray diffraction data.
Buffer	3 μL	2.5 μL	2.0 μL	2.0 μL	1.5 μL	1.0 μL	
Protein	1 μL	1.5 μL	2.0 μL	2.0 μL	2.5 μL	3.0 μL	

Scoring scale: [-] = Clear solution, 1 = Cloudy precipitate, 2 = Gelatinous precipitate, 3 = Spherullites, 4 = Needles, 5 = Planes, 6 = prism, X = Smeared well

Table 3: X-ray diffraction data collection

Crystal data entry	Angle of rotation (Q)	Oscillation (DQ)	Distance (D)	Time (sec)	Observation
1	0	1	50	20	No diffraction
	45	1	50	20	No diffraction
2	0	1	50	20	Diffraction at 2 Å no ice
	45	1	50	20	Diffraction at 2.4 Å no ice
3	0	1	50	60	Diffraction at 2.4Å no ice
	45	1	50	60	Diffraction at 2.4Å no ice

Table 4: Images collected from crystal number 3 at 30 and 60 secs

Images	Start angle (Q)	Oscillation (DQ)	Distance (D)	Time (sec)	Observation
59	45	1	50	30	Diffraction at 2.4 Å, No ice formation
59	45	1	50	60	Diffraction at 1.9 Å No ice formation

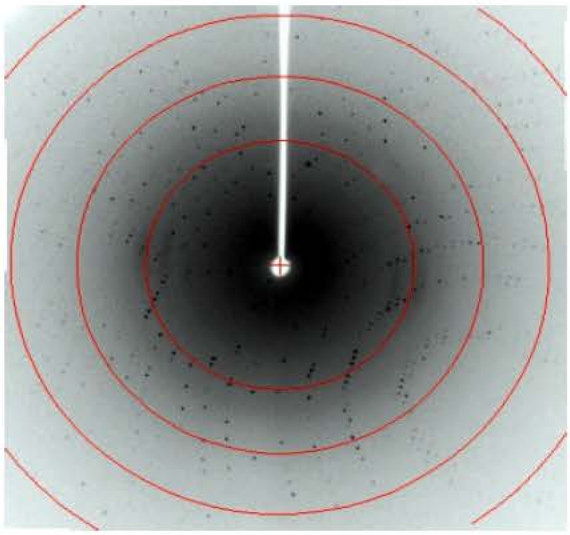

Fig. 1: X-ray diffraction scatter gram of lysozyme crystal form grown in buffer A (0.1 M Na acetate/0.1 M acetic acid pH 4.8, 0.2% Na Azide w/v, 1.1 M NaCl), from data entry 59 = angle of rotation (45°), Oscillation 1, distance 50, time 30 sec)

The X-ray diffraction scattergram was taken for the different data entries as shown in Fig. 1.

Well formed crystals in well plates with buffer protein ratio of 1.5:2.4 μL, given a total volume of 4 μL Fig. 2 were used for the X-ray diffraction.

Figure 3 shows the electron density map of lysozyme active site where the sodium ions and chlorine ions could interact. One side of the active chain is the interaction with the residues such as arginine (Arg) 113 and arginine

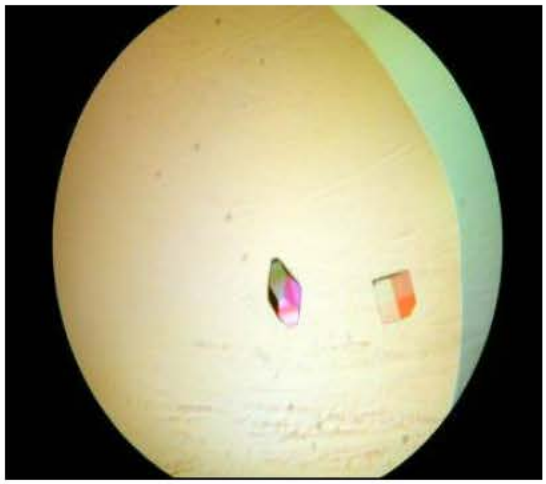

Fig. 2: Lysozyme crystals grown by hanging drop techniques, harvested from buffer A well under growth conditions (0.1 M Na acetate adjusted, 0.02% Na Azide w/v, 1.1 M Na CL adjusted to pH of 4.8 with 0.1 M acetic acid

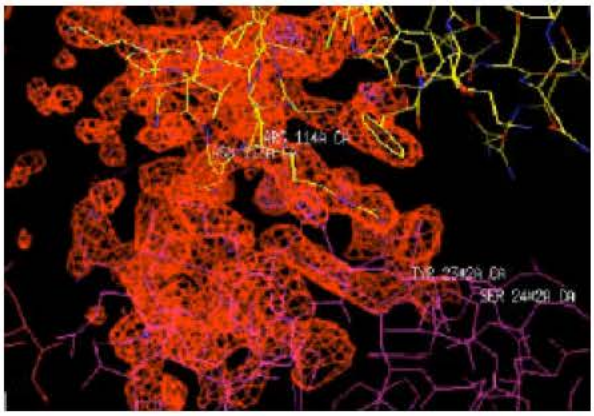

Fig. 3: Electron density maps of lysozyme crystal showing the interaction of atoms on the active site

Table 5: Data collection and refinement

Data collection	Lysozyme crystal Form
Number of crystals	1.0
Unit cell length	37.0900
Unit cell angles	90.000
Unit cell volume (Å^3)	229998.428
Resolution range	22.27-2.20 Å (2.28-1.92 Å) outer
Total number of reflections	27553
Number of unique reflections	6208
Space group	P4$_1$2$_1$2
Mosaicity	0.415
Average redundancy	4.44 (4.36) model
% Completeness	98.7
Rmerge	5.8% (12.5%) model
I/sig (I)	17.7 (8.9)

(Arg) 114 and on the other side of the active site are tyrosine (Tyr 23) and serine (Ser) 24.

The electron density maps shows the active site in lysozyme crystal with the catalytic residues near the glycosidic bond that is cleaved by lysozyme aspartate 52 and glutamic 35 .The aspartate 52 is on the side of the glycosidic bond, whereas the glutamate residue is on the other. These two acidic side chains have markedly different environment. Aspartate 52 is in a distinctly polar environment, where it serves as hydrogen-bond acceptor in a complex network.

DISCUSSION

Although a number of new, higher resolution microscope have been developed, the only method that currently yields reliable structures of macromolecules at atomic resolution is X-ray diffraction from single crystals[15,16] .This technique requires three distinct steps: growing crystal, collecting the X-ray diffraction pattern from the crystal and constructing and refining a structural model to fit the X-ray diffraction pattern[17-19].

The importance of the three-dimensional structures of macromolecules has been widely recognized for many years. Structural molecular biology has become a powerful tool for understanding enzyme function and treatment of diseases[3,10,13,20]. As structure-based drug design has proved its value, the demand for the determination of three-dimensional structures of proteins has increased. However, the bottleneck in three-dimensional structure determination still remains the growth of high-quality protein crystals[19,21]. Many attempts have been made to produce better diffracting crystals by determining the optimum growth conditions (choosing the proper precipitant, buffer concentration and temperature, using different crystallization methods and so on[22,23]. One of the most important experimental parameters in crystal growth is supersaturation, irrespective of the growth method. Supersaturation (S) is defined as S = (C-Ce)/Ce, where, C is the protein concentration and Ce is the protein solubility (with the same precipitant concentration, buffer and temperature)[13,24].

Hen egg-white lysozyme (E.C.3.2.1.17; HEWL) was the first enzyme to have its three-dimensional structure determined[13,25,26] and has become one of the most studied enzymes in structural biology to date. The reason for this is that it can be easily crystallized in various crystal forms, which yield X-ray diffraction data to high resolution and high quality. The use of Hen egg-white lysozyme for the structural studies gave the opportunity to understand the principle of crystallization, X-ray diffraction and the production of high quality crystals using the (vapour

diffusion) hanging drop technique[14,27]. The X-ray diffraction data produced a high outer resolution range Å of the crystal (2.28–1.92 Å), within the $P4_32_12$ space group. The quality of the lysozyme crystal was also evidenced by the percentage completeness (98.7%) and mosaicity of 0.415 that has been reported by others[13,28,29].

The cryocrystallographic techniques are now widely used for X-ray data collection in structure determination of biological macromolecules. Flash cooling of the lysozyme crystal to temperature of 100 K and use of cryoprotectants such as glycerine during mounting of the crystal, reduces radiation damage and increases crystal lifetimes in intense X-ray beams by a factor of ~ 10^3, favourable cases allowing complete diffraction data sets to be collected using a single crystal[14,30]. A search for possible catalytic groups (directly participating in formation or breakage of covalent bonds) has been achieved with lysozymes[7,30,31]. The catalytic residues near the glycosidic bond that is cleaved by lysozyme are aspartate 52 and glutamic 35. The aspartatic acid residue is on one side of the glycosidic linkage, whereas the glutamic acid residue is on the other[7,10,32,34].

Vapour diffusion techniques used in the crystallization study is the most commonly employed methods for growing crystals of macromolecules for X-ray structure determination[26,32,34]. In theory the initial conditions in the droplet are such that the protein is either in a metastable or undersaturated state with respect to crystal nucleation[26,34]. The loss of water serves to both concentrate the protein and the precipitant concentrations within the drop, bringing the protein past the metastable point to nucleation[10,35].

The vapour diffusion technique was shown to be a successful high throughput method for producing high quality crystals from hen egg white lysozyme, with a high resolution of 1.92Å. The high resolution crystal served as a perfect model in structure- drug design studies.

REFERENCES

1. Hirschler, J., 1996. Contaminant effects on protein crystal morphology in different growth environments. Acta Crystallogr. D. Biol. Crystallogr., 52: 806-812.
2. Vaney, M.C., 1996. High-resoluion structure (1.33 A) of a HEW lysozyme tetragonal cyrstal grown in the apcf apparatus. Data and structural comparison with a crytal grown under microgravity from space hab-01 mission. Acta Crystallogr. D. Biol. Crystallogr., 52: 505-517.
3. Holmes, A.M., 1997. Electrophoretic mobility and zeta potential of lysozyme crystals. Acta. Crystallogr. D. Biol. Crystallogr., 53: 456-457.
4. Snell, E.H., 1995. Improvements in lysozyme protein crystal perfection through microgravity growth. Acta Crystallogr. D. Biol. Crystallgr., 51: 1099-1102.
5. Katrusiak A., 1996. Compressibility of lysozyme protein crystals by X-ray diffraction. Acta Crystallogr. D. Biol. Crystallogr., 52: 607-608.
6. Stajanoff, V., 1997. X-Ray topography of tetragonal lysozyme grown by the temperature-controlled technique. Acta Crystallogr. D. Biol. Crystallogr., 53: 588-595.
7. Stryer, L., 1981. Biochemistry (2nd Edn.) W.H. Freeman and Company, New York, pp: 946.
8. Nadarajah, A., 1997. Growth Mechanism of the (110) face of Tetragonal Lysozyme Crystals. Acta Crytallogr. D. Biol. Crystallogr., 53: 524-534.
9. Thomas, B.R., 1996. Heterogeneity determination and purification of commercial hen egg-white lysozyme. Acta Crystallogr. D. Biol. Crystallogr., 52: 776-784.
10. Forsythe, E.L., D.L. Maxwell and M. Pusey, 2002. Vapour diffusion, nucleation rates and reservoir to crystallization volume ratio. Acta Crystallographica., 58: 1601-1605.
11. Vekilov, P.G., L.A. Monaco, B.R. Thomas, V. Stojanoff and F. Rosenberger., 1996. Repartitioning of NaCl and protein impurities in lysozyme crystallization. Acta Crystallogr. D. Biol. Crystallogr., 52: 785-798.
12. Rao, S.T., 2001. Studies on monoclinic hen egg-white lysozyme. IV. X-ray refinement at resolution and a comparison of the variable regions in the polymorphic. Acta crystallgr. D. Biol. Crystallogr., 52: 170-175.
13. Yoshizaki, T., T.S. Noriyuki, N. Tanaka and S. Yoda, 2001. Systemic analysis of supersaturation and lysozyme crystal quality. Acta Crystallogr. D. Biol. Crystallogr., 5: 1621-1629.
14. Garman, E.F. and T.R. Schneider, 1997. Macromolecular crystallography. J. Applied Crystallogr., 30: 211-237.
15. Ducruix, A. and R. Giege, 1992. Crystallization of Nucleic Acids and Proteins, a Practical Approach, Oxford University Press, Oxford, pp: 345.
16. Saijo, S., Y. Yamada, T. Sato, N. Tanaka, T. Matsui and G. Sazaki, 2005. Structural consequences of hen egg-white lysozyme orthorhombic crystal growth in a high magnetic field: validation of X-ray diffraction intensity, conformational energy searching and quantitative analysis of B factors and mosaicity. Acta Crystallogr. D. Biol. Crystallogr., 61: 207-217.
17. Drenth, J., 1994. Principles of Protein X–ray Crystallography, Springler-Verlag, New York, pp: 288.

18. Harata, K. and T. Akiba, 2004. Phase transition of triclinic hen egg-white lysozyme crystal associated with sodium binding. Acta Crystallogr. D. Biol. Crystallogr., 60: 630-637.
19. Yoshizaki, I., A. Kadowaki, Y. Limura, N. Igarashi, S. Yoda and H. Komatsu, 2004. Impurity effects on lysozyme crystal growth. J. Synchrotron. Radiat., 11: 30-33.
20. Weissenborn, R., K. Diederichs, W. Welte, G. Maret and T. Gisler, 2005. Non-thermal microwave effects on protein dynamics? An X-ray diffraction study on tetragonal lysozyme crystals. Acta Crystallogr. D. Biol. Crystallogr., 55: 163-172.
21. Ho, J.G. and A.P. Middelberg, 2003. The influence of molecular variation on protein interactions. Biotechnol. Bioeng., 84: 611-6.
22. Majeed, S., G. Ofek, A. Belachew, C.C. Huang, T. Zhou and P.D. Kwong, 2003. Enhancing protein crystallization through precipitant synergy. Structure, 11: 1061-1070.
23. Tachibana, M., H. Koizumi, K. Izumi, K. Kajiwara, K. Kojima, 2003. Identification of dislocations in large tetragonal hen egg-white lysozyme crystals by synchrotron white-beam topography. J. Synchrotron Radiat., 10: 416-420.
24. Manno, M., C. Xiao, D. Bulone, V. Martorana and P.L. San Biagio, 2003. Thermodynamic instability in supersaturated lysozyme solutions: Effect of salt and role of concentration fluctuations. Phys. Rev. E. Stat. Nonlin. Soft Matter Phys., 68: 011904.
25. Harata, K. and M. Muraki, 1997. X-ray structure of turkey-egg lysozyme complex with tri-N-acetylchitotriose. Lack of binding ability at subsite A. Acta Crystallgr. D. Biol. Crystallogr., 53: 650-657.
26. Rafaee, M., T. Tezuka, K. Akasaka and M.P. Williamson, 2003. Pressure-dependent changes in the solution structure of hen-white lysozyme. J. Mol. Biol., 327: 857-865.
27. Kawamura, S, M. Eto, T. Imoto, S. Ikemizu, T. Araki and T. Torikata, 2004. Functional and structural sffects of mutagenic replacement of Asn 37 at subunit F on the lysozyme-catalyzed reaction. Biosci. Biotechnol. Biochem., 68: 593-601.
28. Judge, A.R., E.L. Forsythe and M. Pusey, 1998. The effect of protein impurities on lysozyme crystal growth. Biotechnol. Bioeng., 48: 776-785.
29. Penkova, A., N. Chayen, E. Saridakis and C.N. Naney, 2002. Nucleation of protein crystals in a wide continuous supersaturation gradient. Acta Crystallographica. Section, 58: 1606-1610.
30. Kriminski, S., C.L. Caylor, M.C. Nonato and R.E. Thorne, 2002. Flash-cooling and annealing of protein crystals. Acta Crystallographica. Section, 58: 459-471.
31. Dong, X.Y., Y. Huang and Y. Sun, 2004. Refolding kinetics of denatured-reduced lysozyme in the presence of folding aids. J. Biotechnol., 114: 135-142.
32. Forsythe, E.L., 1997. Crystallization of chicken egg-white lysosyme from ammonium sulphate. Acta Crystallogr. D. Biol. Crystallogr., 53: 456-457.
33. Toshima, G, S. Kawamura, T. Araki and T. Torikata, 2003. Histidine-114 at subsites E and F can explain the characteristic enzymatic activity of guinea hen egg-white lysozyme. Biosci. Biotechnol. Biochem., 67: 540-546.
34. Sethuraman, A. and G. Belfort, 2005. Protein structural perturbation and aggregation on homogeneous surfaces. Biophys. J., 88: 1322-1333.
35. Peters, N.C., D.H. Hamilton and P.A. Bretscher, 2005. Analysis of cytokine-producing. Th cells from hen egg lysozyme-immunized mice reveals large numbers of specific for cryptic peptides and different repertoires among different Th populations. Eur. J. Immumol., 35: 56-65.